

Toward Adaptive Tracking and Communication via an Airborne Maneuverable Bi-Static ISAC System

Mingliang Wei, Ruoguang Li, *Member, IEEE*, Li Wang, *Senior Member, IEEE*, Lianming Xu, *Member, IEEE*, Zhu Han, *Fellow, IEEE*

Abstract—In this letter, we propose an airborne maneuverable bi-static integrated sensing and communication (ISAC) system where both the transmitter and receiver are unmanned aerial vehicles (UAVs). By timely forming a dynamic bi-static range based on the motion information of the target, such a system can provide an adaptive two-dimensional (2D) tracking and communication services. Towards this end, a trajectory optimization problem for both transmit and receive UAV is formulated to achieve high-accurate motion state estimation by minimizing the time-variant Cramér–Rao bound (CRB), subject to the sufficient communication signal-to-noise ratio (SNR) to maintain communication channel prediction error. Then we develop an efficient approach based on the successive convex approximation (SCA) technique and the S-procedure to address the problem. Numerical results demonstrate that our proposed airborne maneuverable bi-static ISAC system is able to obtain higher tracking accuracy compared with the static or semi-dynamic ISAC system.

Index Terms—integrated sensing and communication (ISAC), unmanned aerial vehicle, extended Kalman filtering, adaptive tracking and communication.

I. INTRODUCTION

Integrated sensing and communication (ISAC) has emerged as one of key enablers in the sixth-generation (6G) mobile communication, in which the radar sensing and communication (S&C) functionalities seamlessly share the wireless resources and hardware in a single system to achieve simultaneous S&C services in many applications, such as autonomous driving, emergency rescue, etc. [1]. However, the traditional ISAC system based on terrestrial infrastructure may face S&C performance degradation due to the obstacles that cause line-of-sight (LoS) blockage. Recently, unmanned aerial vehicles (UAVs) are envisioned as promising ISAC platforms, which

This work was supported in part by the National Natural Science Foundation of China under Grants U2066201, 62301157, and 62171054, in part by the Natural Science Foundation of Jiangsu Province of China under Project BK20230823, in part by the Fundamental Research Funds for the Central Universities under Grant No.24820232023YQTD01, in part by the Interdisciplinary Team Project Funds for the Double First-Class Construction Discipline under Grant No. 2023SYLTD06, and in part by the Fundamental Research Funds for the Central Universities under Grant No. 2024RC06. (*Mingliang Wei and Ruoguang Li are co-first authors.*)(*Corresponding author: Li Wang.*)

Mingliang Wei and Li Wang are with the School of Computer Science (National Pilot Software Engineering School), Beijing University of Posts and Telecommunications, Beijing 100876, China (e-mail: {weiml, liwang}@bupt.edu.cn).

Ruoguang Li is with the College of Information Science and Engineering, Hohai University, Changzhou 213200, China (e-mail: ruoguangli@hhu.edu.cn).

Lianming Xu is with School of Electronic Engineering, Beijing University of Posts and Telecommunications, Beijing 100876, China (e-mail: xulianming@bupt.edu.cn).

Zhu Han is with the Department of Electrical and Computer Engineering, University of Houston, Houston, TX 77004 USA, and also with the Department of Computer Science and Engineering, Kyung Hee University, Seoul 446-701, South Korea (e-mail: hanzhu22@gmail.com).

can provide enhanced S&C services from sky by exploiting high mobility and strong LoS propagation [2].

The prior works about UAV-enabled ISAC system mainly focused on the monostatic topology with a single ISAC transceiver and static target. In particular, the authors in [3] proposed a single UAV-assisted adaptable ISAC (AISAC) mechanism to improve the wireless resource utilization by flexibly adjusting the S&C duration. In [4], the UAV trajectory and beamforming were jointly designed to balance the tradeoff between S&C performance. It is worth noting that the main disadvantage of the monostatic ISAC system is the self-interference from the transmit array to receive array. Therefore, recent works began to study the bi-static and multi-static UAV-enabled ISAC system where different UAVs play roles as separately deployed transmitters and receivers. In particular, the authors in [5] jointly considered the trajectory of UAVs, user association, and beamforming design to maximize the communication rate while ensuring the sensing beampattern gain. The authors in [6] jointly optimized UAV scheduling and resource allocation in a multi-UAV ISAC system to maximize the worst-case communication rate under the constraint of radar MI. When it comes to moving targets (MTs), the motion parameters should be timely predicted, which relies more on the good tracking ability. In [7], the authors proposed an alternating path planning and resource allocation (APRA) algorithm to minimize the Cramér–Rao bounds (CRB) for MT state estimation in the multi-UAV ISAC network. In [8], the user association and multi-UAV trajectories were jointly optimized to achieve more reliable communication services and more accurate MT tracking. Although the above works exploited cooperation among UAVs to enhance the tracking performance, they only considered a *semi-dynamic* ISAC system, which solely optimized the trajectories of transmit UAVs, assuming that the location of the receiver is fixed. However, the maneuverability of UAVs intrinsically makes it possible that both the transmitter and receiver can dynamically adjust their location to improve the tracking performance by providing more design degree of freedom (DoF).

Motivated by the aforementioned studies, we investigate an adaptive tracking and communication mechanism via an airborne maneuverable bi-static ISAC system. The main contributions are summarized as follows:

- We propose an airborne maneuverable bi-static ISAC system in which the transmit and receive UAVs timely change locations to form a dynamic bi-static range for simultaneous two-dimensional (2D) motion estimation and data transmission with a ground MT. The motion parameters, which involves location and velocity, are estimated by the extended Kalman filter (EKF) algorithm.
- A joint transmit and receive UAV trajectory optimiza-

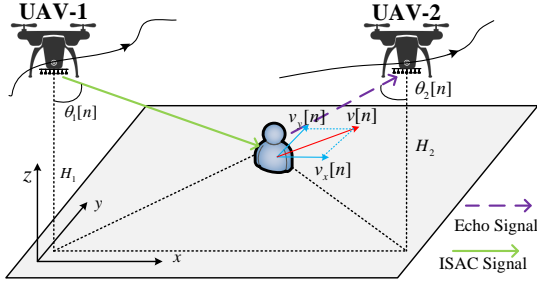


Fig. 1. Airborne maneuverable bi-static ISAC system.

tion problem is formulated to minimize the time-variant CRB while meeting the communication requirement. To address the non-convex problem, we propose a method using successive convex approximation (SCA) and the S-procedure for convex transformation and obtain a sub-optimal solution.

- Simulation results show that the proposed airborne maneuverable bi-static ISAC system can introduce more design DoF compared to the semi-dynamic ISAC system, and achieve superior tracking performance while ensuring communication requirement.

II. SYSTEM MODEL AND PROBLEM FORMULATION

As shown in Fig. 1, we consider an airborne maneuverable bi-static ISAC system, which consists of a transmit UAV, denoted by UAV-1, a receive UAV, denoted by UAV-2, and a single-antenna ground MT. In other words, UAV-1 and UAV-2 play as movable transmitter and receiver, respectively, geographically forming a dynamic bi-static range to adaptively track and communication¹. Additionally, we assume that UAV-1 and UAV-2 are equipped with uniform linear array (ULA) of N_t transmit antennas and N_r receive antennas, respectively, both of which are vertically placed towards the ground [4].

Without loss of generality, we assume that the whole flight period of UAV is T , which is divided into N time slots with duration $\Delta T = T/N$, indexed by $n \in \mathcal{N} = \{1, 2, \dots, N\}$. ΔT is short enough, during which the states of UAVs and MT keep approximately constant. Furthermore, we consider a 3D Cartesian coordinate system where UAV's flight altitude is fixed with the height $H_m, m \in \{1, 2\}$. Let $\mathbf{q}_1[n] = (x_1[n], y_1[n])^T$, $\mathbf{q}_2[n] = (x_2[n], y_2[n])^T, \forall n \in \mathcal{N}$ denote the horizontal locations of UAV-1 and UAV-2, respectively, and $\mathbf{u}[n] = (x[n], y[n])^T$ denotes the location of MT. Besides, the angle of departure (AoD) at UAV-1 or angle of arrival (AoA) at UAV-2 is $\theta_m[n] = \frac{180}{\pi} \arccos(\frac{H_m}{d_m})$, $d_m[n] = \sqrt{\|\mathbf{q}_m[n] - \mathbf{u}[n]\|^2 + H_m^2}$ is the distance between UAVs and MT, and $v_x[n], v_y[n]$ are the components of MT velocity in (x, y) directions at time slot n , respectively. We assume that MT is moving at an approximately constant speed, and then the state evolution model in time slot n can be given by

$$x[n] = x[n-1] + v_x[n-1]\Delta T + \omega_x, \quad (1)$$

$$y[n] = y[n-1] + v_y[n-1]\Delta T + \omega_y, \quad (2)$$

$$v_x[n] = v_x[n-1] + \omega_{v_x}, \quad (3)$$

$$v_y[n] = v_y[n-1] + \omega_{v_y}, \quad (4)$$

¹Our model can be extended to multi-UAV ISAC with three-dimensional (3D) trajectory optimization, which will be considered in our future work.

where $\omega_x \sim \mathcal{N}(0, \sigma_x^2)$, $\omega_y \sim \mathcal{N}(0, \sigma_y^2)$, $\omega_{v_x} \sim \mathcal{N}(0, \sigma_{v_x}^2)$ and $\omega_{v_y} \sim \mathcal{N}(0, \sigma_{v_y}^2)$ are the model transition noises, respectively.

A. Communication Model

The air-to-ground (A2G) communication channel from the UAV-1 to MT is adopted by probabilistic LoS channel model, in which the LoS probability can be expressed as $\mathbb{P}(\text{LoS}, \theta_1[n]) = [1 + e_1 \exp(-e_2(\theta_1[n] - e_{11}))]^{-1}$, where e_1 and e_2 are the environment-related parameters. Therefore, the communication channel vector from the UAV-1 to MT in time slot n is given by $\mathbf{h}[n] = \sqrt{\beta_d[n]d_1^{-\alpha}[n]\mathbf{a}(\theta_1[n])}$, where $\beta_d[n] = \beta_0[\mathbb{P}(\text{LoS}, \theta_1[n]) + (1 - \mathbb{P}(\text{LoS}, \theta_1[n]))\varepsilon]$ is the channel gain with ε being the attenuation effect of the NLoS channel. $d_1[n] = \sqrt{\|\mathbf{q}_1[n] - \mathbf{u}[n]\|^2 + H_1^2}$ is the distance from UAV-1 to MT, β_0 represents the channel gain at the reference distance 1 meter, and α is the path loss exponent. $\mathbf{a}(\theta_1[n]) = \frac{1}{\sqrt{N_t}}[1, \dots, e^{j2\pi d/\lambda(N_t-1)\cos\theta_1[n]}]^T$ is the transmit steering vector, where λ is the carrier wavelength, $d = \lambda/2$ is inter-element spacing. Accordingly, the received signal at the MT in time slot n can be given as

$$c(n, t) = \sqrt{P_t}\mathbf{h}^H[n]\mathbf{f}[n]s(n, t) + n_c(n, t), \quad (5)$$

where $t \in (0, \Delta T)$ is a time instant within time slot n . P_t is the transmit power. $\mathbf{f}[n] \in \mathbb{C}^{N_t \times 1}$ is the transmit beamforming vector, and $s(n, t)$ is the information-bearing signal, $n_c(n, t)$ is the additive white Gaussian noise (AWGN) with zero mean and variance σ_c^2 . Therefore, the received signal-to-noise ratio (SNR) in time slot n is written as

$$\gamma[n] = \frac{P_t|\mathbf{h}^H[n]\mathbf{f}[n]|^2}{\sigma_c^2}. \quad (6)$$

B. Radar Sensing Model

For the radar sensing model, the reflected echo signal received at UAV-2, expressed as

$$\mathbf{r}(n, t) = \xi\mathbf{b}(\theta_2[n])\mathbf{a}^H(\theta_1[n])\mathbf{f}[n]s(n, t - \tau[n])e^{j2\pi f_d t} + \mathbf{n}_r(n, t), \quad (7)$$

where $t \in (0, \Delta T)$ is a time instant within time slot n , ξ and f_d are the complex-valued reflection coefficient and the Doppler frequency, respectively. $\tau[n]$ is the time delay from UAV-1 to UAV-2 after reflecting by MT. $\mathbf{b}(\theta_2[n])$ is the receive steering vector, and $\mathbf{n}_r(n, t) \sim \mathcal{N}(0, \sigma_r^2\mathbf{I}_{N_r})$ is the noise vector. Furthermore, the UAV-2 obtains the time delay $\tau[n] = \frac{1}{c}\sum_{m=1}^2 d_m[n] + z_\tau[n] = \sum_{m=1}^2 (\tau_m[n] + z_{\tau, m}[n])$ by performing the matched-filtering, where c is the speed of light. $\tau_m[n]$ is the time delay from UAVs to MT. $z_{\tau, m}[n] \sim \mathcal{N}(0, \sigma_{\tau, m}^2[n])$ is the time delay measurement noise term, where the corresponding variance is $\sigma_{\tau, m}^2[n] = \frac{a_\tau^2\sigma_r^2(\|\mathbf{q}_m[n] - \mathbf{u}[n]\|^2 + H_m^2)^2}{GP_t N_t N_r \xi}$, where G is the matched-filtering gain, a_τ is the constant parameter related to the system configuration [9].

C. State Evolution and EKF Tracking

Considering the time-delay measurement is nonlinear, we proposed the tracking scheme based on the EKF method. Let $\mathbf{x}[n] = [x[n], y[n], v_x[n], v_y[n]]^T$ and $\mathbf{y}[n] = [\tau_1[n], \tau_2[n]]^T$ denote the state vector and measurement vector at time slot

n , respectively. Accordingly, the state evolution model and measurement model can be written as

$$\begin{cases} \text{Evolution model: } \mathbf{x}[n] = \mathbf{G}[n]\mathbf{x}[n-1] + \boldsymbol{\omega}[n], \\ \text{Measurement model: } \mathbf{y}[n] = \mathbf{e}(\mathbf{x}[n]) + \mathbf{z}[n], \end{cases} \quad (8)$$

where $\mathbf{G}[n]$ is the state transition matrix expressed as

$$\mathbf{G}[n] = \begin{bmatrix} 1 & 0 & \Delta T & 0 \\ 0 & 1 & 0 & \Delta T \\ 0 & 0 & 1 & 0 \\ 0 & 0 & 0 & 1 \end{bmatrix}. \quad (9)$$

Moreover, $\boldsymbol{\omega}[n] = (\omega_x, \omega_y, \omega_{v_x}, \omega_{v_y})^T$ is state transition noise vector with the covariance matrices $\mathbf{Q}[n] = \text{diag}(\sigma_x^2, \sigma_y^2, \sigma_{v_x}^2, \sigma_{v_y}^2)$, and $\mathbf{z}[n] = (z_{\tau,1}[n], z_{\tau,2}[n])^T$ is the measurement noise vector with covariance matrices $\mathbf{R}[n] = \text{diag}(\sigma_{\tau,1}^2[n], \sigma_{\tau,2}^2[n])$. Besides, the Jacobian matrix of $\mathbf{e}(\cdot)$ can be derived as

$$\mathbf{E}[n] = \begin{bmatrix} \frac{x[n]-x_1[n]}{cd_1[n]} & \frac{y[n]-y_1[n]}{cd_1[n]} & 0 & 0 \\ \frac{x[n]-x_2[n]}{cd_2[n]} & \frac{y[n]-y_2[n]}{cd_2[n]} & 0 & 0 \end{bmatrix}. \quad (10)$$

The EKF includes the time update phase and the measurement update phase, which are summarized as follows

$$\hat{\mathbf{x}}[n|n-1] = \mathbf{G}[n]\hat{\mathbf{x}}[n-1], \quad (11)$$

$$\mathbf{M}[n|n-1] = \mathbf{G}[n-1]\mathbf{M}[n-1]\mathbf{G}[n-1]^H + \mathbf{Q}[n], \quad (12)$$

$$\mathbf{K}[n] = \mathbf{M}[n|n-1]\mathbf{E}[n]^H(\mathbf{R}[n] + \mathbf{E}[n]\mathbf{M}[n|n-1]\mathbf{E}[n]^H)^{-1}, \quad (13)$$

$$\hat{\mathbf{x}}[n] = \hat{\mathbf{x}}[n|n-1] + \mathbf{K}[n](\mathbf{y}[n] - \mathbf{e}(\hat{\mathbf{x}}[n|n-1])), \quad (14)$$

$$\mathbf{M}[n] = (\mathbf{I} - \mathbf{K}[n]\mathbf{E}[n])\mathbf{M}[n|n-1]. \quad (15)$$

According to the MT prediction state obtained from time slot $n-1$ using (11) and (12), the equivalent channel in time slot n can be expressed as

$$\hat{\mathbf{h}}[n|n-1] = \sqrt{\hat{\beta}_d[n|n-1]\hat{d}_1^{-\alpha}[n|n-1]}\mathbf{a}(\hat{\theta}_1[n|n-1]), \quad (16)$$

where $\hat{\beta}_d[n|n-1]$, $\hat{d}_1[n|n-1]$, and $\hat{\theta}_1[n|n-1]$ are the predicted communication channel gain, distance from UAV-1 to MT and AoD, respectively. Since the prediction uncertainty in (12) and the prediction communication channel for optimizing the UAV trajectory in time slot n is only based on EKF time update phase, the channel prediction in (16) is also inaccurate. We assume that $\|\Delta\mathbf{h}[n|n-1]\|^2 \leq \epsilon^2$ holds for the communication channel prediction error $\Delta\mathbf{h}[n|n-1]$, where $\epsilon^2 = \|\psi\mathbf{M}[n|n-1]\|^2$ and ψ can be obtained via Monte Carlo simulation [10]. Then we have

$$\mathbf{h}[n] = \hat{\mathbf{h}}[n|n-1] + \Delta\mathbf{h}[n|n-1], \quad (17)$$

and the received SNR can be rewritten accordingly as

$$\hat{\gamma}[n|n-1] = \frac{P_t |(\hat{\mathbf{h}}[n|n-1] + \Delta\mathbf{h}[n|n-1])^H \mathbf{f}[n]|^2}{\sigma_c^2}, \quad (18)$$

where $\mathbf{f}[n] = \hat{\mathbf{h}}[n|n-1] + \Delta\mathbf{h}[n|n-1]$ is based on the predicted AoD. We adopt the CRB to characterize the sensing performance [8]. Specifically, the CRB of MT location can be expressed as $\text{CRB}_{\mathbf{u}[n]} = \mathbf{P}_{\mathbf{u}[n]}^{-1}$, where $\mathbf{P}_{\mathbf{u}[n]} = \mathbf{C}[n]^H \mathbf{R}^{-1}[n] \mathbf{C}[n]$ is the Fisher information matrix (FIM), $\mathbf{C}[n]$ is the Jacobian matrix of $\mathbf{e}(\cdot)$ only with respect to $\mathbf{u}[n]$,

i.e., $\mathbf{C}[n] = \mathbf{E}[n]_{(1:2,1:2)}$. Therefore, the CRB with respect to the MT location is given as²

$$\text{CRB}_{\mathbf{u}[n]} = \frac{P_b + P_a}{P_a P_b - P_c^2}, \quad (19)$$

where

$$P_a = \sum_{m=1}^2 \frac{(\boldsymbol{\eta}_1^T(\mathbf{u}[n] - \mathbf{q}_m[n]))^2}{c^2 \sigma_{\tau,m}^2[n] (\|\mathbf{u}[n] - \mathbf{q}_m[n]\|^2 + H_m^2)}, \quad (20)$$

$$P_b = \sum_{m=1}^2 \frac{(\boldsymbol{\eta}_2^T(\mathbf{u}[n] - \mathbf{q}_m[n]))^2}{c^2 \sigma_{\tau,m}^2[n] (\|\mathbf{u}[n] - \mathbf{q}_m[n]\|^2 + H_m^2)}, \quad (21)$$

$$P_c = \sum_{m=1}^2 \frac{\boldsymbol{\eta}_1^T(\mathbf{u}[n] - \mathbf{q}_m[n])\boldsymbol{\eta}_2^T(\mathbf{u}[n] - \mathbf{q}_m[n])}{c^2 \sigma_{\tau,m}^2[n] (\|\mathbf{u}[n] - \mathbf{q}_m[n]\|^2 + H_m^2)}, \quad (22)$$

where $\boldsymbol{\eta}_1 = [1, 0]^T$ and $\boldsymbol{\eta}_2 = [0, 1]^T$, respectively. Our goal is to minimize the CRB by optimizing the trajectory of UAV-1 and UAV-2 while meeting the communication demands. Accordingly, the optimization problem can be formulated as

$$\min_{\{\mathbf{q}_m[n]\}} \text{CRB}_{\mathbf{u}[n]}(\{\mathbf{q}_m[n]\}) \quad (23a)$$

$$\text{s.t. } \hat{\gamma}[n|n-1] \geq \gamma_c, \|\Delta\mathbf{h}[n|n-1]\|^2 \leq \epsilon^2, \quad (23b)$$

$$\|\mathbf{q}_m[n+1] - \mathbf{q}_m[n]\| \leq V_{\max} \Delta T, m \in \{1, 2\}, \quad (23c)$$

$$\|\mathbf{q}_1[n] - \mathbf{q}_2[n]\| \geq d_{\min}, \quad (23d)$$

where $\mathbf{q}_m[n]$ is the location of UAV in time slot n , γ_c is the given SNR threshold, d_{\min} is the safe flight distance, V_{\max} is the maximum UAV speed. In problem (23), (23b) guarantees the communication requirements, (23c) and (23d) denote the mobility constraints and collision avoidance constraints of UAV, respectively.

III. PROPOSED SOLUTION

Considering the actual location of MT is unknown when optimizing UAV trajectory in time slot n , we utilize $\hat{\mathbf{u}}[n|n-1]$ to replace the actual location $\mathbf{u}[n]$. Therefore, the objective function (23a) can be reformulated as

$$\text{CRB}_{\hat{\mathbf{u}}[n|n-1]} = \frac{\hat{P}_a + \hat{P}_b}{\hat{P}_a \hat{P}_b - \hat{P}_c^2}, \quad (24)$$

where

$$\hat{P}_a = \sum_{m=1}^2 \frac{(\boldsymbol{\eta}_1^T(\hat{\mathbf{u}}[n|n-1] - \hat{\mathbf{q}}_m[n|n-1]))^2}{c^2 \sigma_{\tau,m}^2[n] (\|\hat{\mathbf{u}}[n|n-1] - \hat{\mathbf{q}}_m[n|n-1]\|^2 + H_m^2)}, \quad (25)$$

$$\hat{P}_b = \sum_{m=1}^2 \frac{(\boldsymbol{\eta}_2^T(\hat{\mathbf{u}}[n|n-1] - \hat{\mathbf{q}}_m[n|n-1]))^2}{c^2 \sigma_{\tau,m}^2[n] (\|\hat{\mathbf{u}}[n|n-1] - \hat{\mathbf{q}}_m[n|n-1]\|^2 + H_m^2)}, \quad (26)$$

$$\hat{P}_c = \sum_{m=1}^2 \left\{ \frac{\boldsymbol{\eta}_1^T(\hat{\mathbf{u}}[n|n-1] - \hat{\mathbf{q}}_m[n|n-1])}{c^2 \sigma_{\tau,m}^2[n] \sqrt{\|\hat{\mathbf{u}}[n|n-1] - \hat{\mathbf{q}}_m[n|n-1]\|^2 + H_m^2}} \cdot \frac{\boldsymbol{\eta}_2^T(\hat{\mathbf{u}}[n|n-1] - \hat{\mathbf{q}}_m[n|n-1])}{\sqrt{\|\hat{\mathbf{u}}[n|n-1] - \hat{\mathbf{q}}_m[n|n-1]\|^2 + H_m^2}} \right\}. \quad (27)$$

It can be observed that due to the non-convexity of the objective function in (24) and the constraints in (23b) and (23d), problem (23) is NP-hard and cannot be solved by conventional convex optimization methods. Therefore, we apply the SCA and the S-procedure method to tackle these difficulties. We

²Since the velocity of MT can be calculated from its location, we presents the CRB with respect to the MT location as the tracking performance metric.

first transform the non-convex objective function (24) into a convex one. Specifically, by applying the first-order Taylor expansion of $\text{CRB}_{\hat{\mathbf{u}}[n|n-1]}$ as global lower bound, we have

$$\begin{aligned} \text{CRB}_{\hat{\mathbf{u}}[n|n-1]} &\triangleq f(\mathbf{q}_1[n], \mathbf{q}_2[n]) \geq f(\mathbf{q}_1^k[n], \mathbf{q}_2^k[n]) \\ &+ \sum_{m=1}^2 \nabla f_{\mathbf{q}_m}[n](\mathbf{q}_1^k[n], \mathbf{q}_2^k[n])^T (\mathbf{q}_m[n] - \mathbf{q}_m^k[n]), \end{aligned} \quad (28)$$

where $\mathbf{q}_1^k[n], \mathbf{q}_2^k[n]$ denote the locations of UAV-1 and UAV-2 at time slot n in the k -th iteration of SCA, respectively. Next, to address the remaining non-convexity of constraints (23b), we adopt the S-procedure method to transform it into a more tractable form. Specifically, (23b) can be rewritten as linear matrix inequalities (LMIs) with following lemma.

Lemma. (S-procedure [11]:) Let a function $f_u(\mathbf{x})$ be defined as following form

$$f_u(\mathbf{x}) = \mathbf{x}^H \mathbf{B}_u \mathbf{x} + 2\Re\{\mathbf{b}_u^H \mathbf{x}\} + b_u, u \in \{1, 2\}, \quad (29)$$

where $\mathbf{x} \in \mathbb{C}^{M \times 1}$, $\mathbf{B}_u \in \mathbb{C}^{M \times M}$, $\mathbf{b}_u \in \mathbb{C}^{M \times 1}$, and $b_u \in \mathbb{R}^{1 \times 1}$. Then the implication $f_1(\mathbf{x}) \leq 0 \Rightarrow f_2(\mathbf{x}) \leq 0$ holds if and only if exist $\zeta \geq 0$ such that

$$\zeta \begin{bmatrix} \mathbf{B}_1 & \mathbf{b}_1 \\ \mathbf{b}_1^H & b_1 \end{bmatrix} - \begin{bmatrix} \mathbf{B}_2 & \mathbf{b}_2 \\ \mathbf{b}_2^H & b_2 \end{bmatrix} \succeq \mathbf{0}, \quad (30)$$

which proves that there exists a point $\hat{\mathbf{x}}$ such that $f_u(\hat{\mathbf{x}}) < 0$.

Based on the above lemma, constraint (23b) can be expanded as

$$\begin{aligned} \Delta \mathbf{h}^H[n|n-1] \left(-1 - \frac{1}{\gamma_c} \right) \Delta \mathbf{h}[n|n-1] \\ + 2\Re\left\{ \hat{\mathbf{h}}^H[n|n-1] \left(-1 - \frac{1}{\gamma_c} \right) \Delta \mathbf{h}[n|n-1] \right\} \end{aligned} \quad (31)$$

$$\begin{aligned} + \hat{\mathbf{h}}^H[n|n-1] \left(-1 - \frac{1}{\gamma_c} \right) \hat{\mathbf{h}}[n|n-1] + \sigma_c^2 \leq 0, \\ \|\Delta \mathbf{h}[n|n-1]\|^2 \leq \epsilon^2, \forall n \in \mathcal{N}, \end{aligned} \quad (32)$$

where (32) can be further rewritten as

$$\Delta \mathbf{h}^H[n|n-1] \mathbf{I}_{N_t} \Delta \mathbf{h}[n|n-1] - \epsilon^2 \leq 0, \forall n \in \mathcal{N}. \quad (33)$$

Correspondingly, constraint (23b) can be expressed as the following LMI

$$\begin{aligned} \begin{bmatrix} \mathbf{I}_{N_t} & \\ \hat{\mathbf{h}}^H[n|n-1] & \end{bmatrix} \left\{ -1 - \frac{1}{\gamma_c} \right\} \begin{bmatrix} \mathbf{I}_{N_t} & \\ \hat{\mathbf{h}}^H[n|n-1] & \end{bmatrix}^H \\ + \begin{bmatrix} \mu[n] \mathbf{I}_{N_t} & \mathbf{0}_{N_t} \\ \mathbf{0}_{N_t}^H & -\mu[n] \epsilon^2 - \sigma_c^2 \end{bmatrix} \succeq \mathbf{0}, \end{aligned} \quad (34)$$

$\mu[n] \geq 0, \forall n \in \mathcal{N}$.

Similar to (28), we finally perform the first-order Taylor expansion of (23d) with respect to $\mathbf{q}_1[n]$ and $\mathbf{q}_2[n]$ at the given point $\mathbf{q}_1^k[n]$ and $\mathbf{q}_2^k[n]$, which is expressed as

$$\begin{aligned} \|\mathbf{q}_1[n] - \mathbf{q}_2[n]\|^2 &\geq 2(\mathbf{q}_1^k[n] - \mathbf{q}_2^k[n])^T (\mathbf{q}_1[n] - \mathbf{q}_2[n]) \\ &- \|\mathbf{q}_1^k[n] - \mathbf{q}_2^k[n]\|^2 \geq d_{\min}^2. \end{aligned} \quad (35)$$

Denoting the last term of the right-hand side (RHS) in (28) as $F(\mathbf{q}_1[n], \mathbf{q}_2[n])$, the optimization problem in (23) can be reformulated as

$$\min_{\mathbf{q}_1[n], \mathbf{q}_2[n]} F(\mathbf{q}_1[n], \mathbf{q}_2[n]) \quad (36a)$$

$$\text{s.t.} \quad (23c), (34), (35). \quad (36b)$$

Algorithm 1 : Proposed Algorithm for Solving Problem (23)

- 1: Initialize : set the time slot index $n = 2$, SCA iteration index $k = 1$, maximum iteration k_{\max} , the threshold η , $\mathbf{x}[1], \mathbf{M}[1], \mathbf{q}_1[1], \mathbf{q}_2[1]$
 - 2: **repeat**
 - 3: Compute $\hat{\mathbf{x}}[n|n-1]$ by (11) and $\mathbf{M}[n|n-1]$ by (12).
 - 4: **repeat**
 - 5: With $\hat{\mathbf{u}}[n|n-1], \mathbf{q}_1^k[n], \mathbf{q}_2^k[n]$ to solve the problem (36), and denote the optimal solution as $\mathbf{q}_1^{k+1}[n], \mathbf{q}_2^{k+1}[n]$.
 - 6: Update $k = k + 1$.
 - 7: **until** $F^{(k+1)} - F^{(k)} \leq \eta$ or $k \geq k_{\max}$.
 - 8: With $\hat{\mathbf{u}}[n|n-1], \mathbf{q}_1^k[n], \mathbf{q}_2^k[n]$ to obtain $\mathbf{K}[n]$ by (13).
 - 9: With $\hat{\mathbf{y}}[n], \mathbf{K}[n]$ to obtain $\hat{\mathbf{x}}[n], \mathbf{M}[n]$ by (14) and (15).
 - 10: Set $n = n + 1$.
 - 11: **until** $n > N$
-

Problem (36) is a convex optimization problem that can be solved by standard solvers such as CVX [12]. Besides, the details of the proposed method are given in Algorithm 1, and we analyze the complexity of Algorithm 1. At each time slot, the complexity of EKF method is $\mathcal{O}(4^3)$ [8]. Let K_n denote the iteration number in time slot n and the complexity of problem (36) is $\mathcal{O}(K_n 2^{3.5} \log(1/\eta))$. Therefore, the overall complexity of Algorithm 1 is $\mathcal{O}(\sum_{n=1}^N [4^3 + K_n 2^{3.5} \log(1/\eta)])$.

IV. SIMULATION RESULTS

In this section, we present the numerical results to validate the tracking and communication performance of the proposed airborne maneuverable bi-static ISAC system. The following required parameters are used: $T = 15$ s, $\Delta T = 0.5$ s, $e_1 = 25$, $e_2 = 0.112$, $\beta_0 = -60$ dB, $\sigma_c^2 = \sigma_r^2 = -110$ dBm, $P_t = 40$ dBm, and $N_t = N_r = 16$ [8]. For the state transition noises are set $\sigma_x^2 = \sigma_y^2 = 1$ m and $\sigma_{v_x}^2 = \sigma_{v_y}^2 = 0.5$ m/s. The measurement noise $a_\tau = a_f = 1.2 \times 10^{-7}$, $G = 10$. Besides, the initial location of MT is $\mathbf{u}[1] = [100\text{m}, 100\text{m}]^T$ with the velocity of 10 m/s. The initial locations of UAV-1 and UAV-2 are $\mathbf{q}_1[1] = [140\text{m}, 100\text{m}]^T$ and $\mathbf{q}_2[1] = [120\text{m}, 200\text{m}]^T$, respectively. The fixed height of UAVs is set to $H_1 = H_2 = 50$ m. The minimum safe flight distance is $d_{\min} = 40$ m and the maximum UAV speed is $V_{\max} = 20$ m/s.

In Fig. 2, it can be observed that the CRB converges quickly within a few iterations and decreases as P_t increases, which validates the effectiveness of our proposed SCA and S-procedure based algorithm. Fig. 3 illustrates the trajectories of UAVs with the proposed system under different γ_c . It is obvious that the estimated path of MT with our proposed system is almost the same as the real one, which shows a excellent tracking performance. Second, as γ_c increases, UAV-1 flies closer toward the MT to obtain better communication performance. In addition, UAV-2 gradually approaches the MT while maintaining a safe flight distance with UAV-1 to achieve higher precise tracking performance. Besides, when the communication is not considered, i.e., $\gamma_c = 0$, UAV-1 and UAV-2 will keep a farther safety distance.

In Fig.4, we compare our proposed system with the semi-dynamic UAV tracking and communication system. Specifically, the location of the (UAV-2) is fixed at two ordinates,

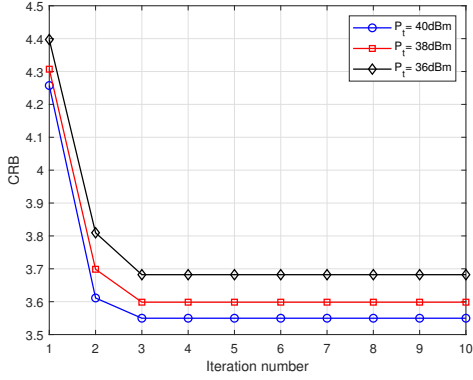


Fig. 2. Convergence performance of the proposed algorithm.

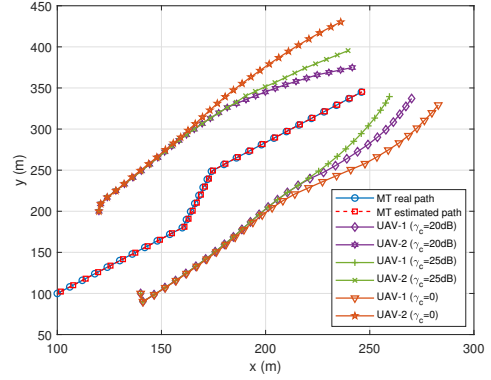


Fig. 3. Trajectories of UAVs with the proposed system under different γ_c .

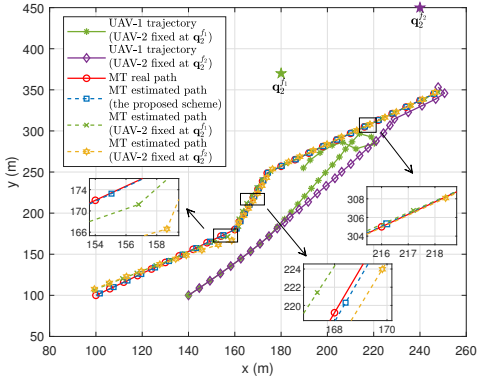


Fig. 4. Trajectory of UAV-1 when UAV-2 is fixed at different locations. ($\mathbf{q}_2^{f1} = [180\text{m}, 370\text{m}]^T$, $\mathbf{q}_2^{f2} = [240\text{m}, 450\text{m}]^T$, $\gamma_c = 25$ dB)

i.e., location1 $\mathbf{q}_2^{f1} = [180\text{m}, 370\text{m}]^T$ and location2 $\mathbf{q}_2^{f2} = [240\text{m}, 450\text{m}]^T$. It can be seen that when the location of UAV-2 varies from \mathbf{q}_2^{f1} to \mathbf{q}_2^{f2} , the estimated path has a different error, both of which are larger than that of our proposed system. Besides, different from the proposed system, in the semi-dynamic ISAC system, UAV-1 continuously approaches the MT, and when the MT moves away from UAV-2, UAV-1 maintains a hovering flight to minimize the CRB. In Fig. 5, we further investigate the CRB and communication SNR versus time slot. It is clearly that compared to the semi-dynamic ISAC system, our proposed system can obtain minimum CRB while meeting the communication requirement over all time slots since we fully utilize the high maneuverability of the UAVs to provide more design DoF.

V. CONCLUSION

In this letter, we proposed an airborne maneuverable bi-static ISAC system where the transmit and receive UAVs dynamically adjust locations to improve tracking and communication performance. We further utilized EKF to predict the 2D motion state of MT and adopted an efficient algorithm based on SCA and the S-procedure to minimize time-variant CRB while meeting the communication requirement. Numerical results demonstrated that compared to the semi-dynamic ISAC system, the proposed airborne maneuverable bi-static ISAC system can significantly decrease the CRB and enhance communication performance.

REFERENCES

[1] H. Zhang et al., "Holographic integrated sensing and communication," *IEEE J. Sel. Areas Commun.*, vol. 40, no. 7, pp. 2114-2130, Jul. 2022.

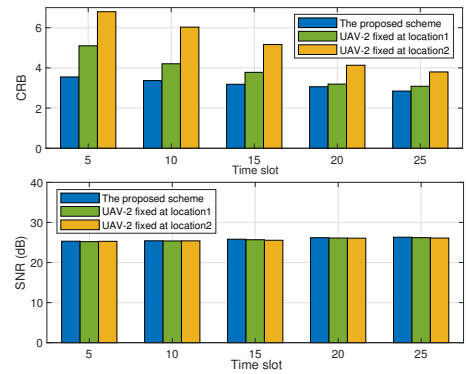


Fig. 5. CRB and communication SNR versus time slot with different motion state of UAV-2. ($\gamma_c = 25$ dB)

- [2] F. Liu et al., "Integrated sensing and communications: toward dual-functional wireless networks for 6G and beyond," *IEEE J. Sel. Areas Commun.*, vol. 40, no. 6, pp. 1728-1767, Jun. 2022.
- [3] C. Deng, X. Fang, and X. Wang, "Beamforming design and trajectory optimization for UAV-empowered adaptable integrated sensing and communication," *IEEE Trans. Wireless Commun.*, vol. 22, no. 11, pp. 8512-8526, Nov. 2023.
- [4] Z. Lyu, G. Zhu, and J. Xu, "Joint maneuver and beamforming design for UAV-enabled integrated sensing and communication," *IEEE Trans. Wirel. Commun.*, vol. 22, no. 4, pp. 2424-2440, Apr. 2023.
- [5] R. Zhang, Y. Zhang, R. Tang, H. Zhao, Q. Xiao, and C. Wang, "A joint UAV trajectory, user association, and beamforming design strategy for multi-UAV assisted ISAC systems," *IEEE Internet Things J.*, early access, 2024.
- [6] X. Liu, Y. Liu, Z. Liu, and T. S. Durrani, "Fair integrated sensing and communication for multi-UAV enabled internet of things: joint 3D trajectory and resource optimization," *IEEE Internet Things J.*, early access, 2023.
- [7] Y. Pan et al., "Cooperative trajectory planning and resource allocation for UAV-enabled integrated sensing and communication systems," *IEEE Trans. Veh. Technol.*, vol. 73, no. 5, pp. 6502-6516, May 2024.
- [8] J. Wu, W. Yuan, and L. Bai, "On the interplay between sensing and communications for UAV trajectory design," *IEEE Internet Things J.*, vol. 10, no. 23, pp. 20383-20395, Dec. 2023.
- [9] F. Liu, W. Yuan, C. Masouros, and J. Yuan, "Radar-assisted predictive beamforming for vehicular links: communication served by sensing," *IEEE Trans. Wirel. Commun.*, vol. 19, no. 11, pp. 7704-7719, Nov. 2020.
- [10] Z. Wei, F. Liu, D. W. Kwan Ng, and R. Schober, "Safeguarding UAV networks through integrated sensing, jamming, and communications," in *Proc. IEEE Int. Conf. Acoust. Speech Signal Process. (ICASSP)*, Singapore city, Singapore, Apr. 2022, pp. 8737-8741.
- [11] R. Li, L. Wang, K. Chen, L. Xu, and A. Fei, "Full-duplex NOMA enabled integrated sensing and communication: joint transmit and receive beamforming optimization," *IEEE Internet Things J.*, vol. 11, no. 16, pp. 27015-27029, Aug. 2024.
- [12] M. Grant and S. Boyd. *CVX: MATLAB Software for Disciplined Convex Programming, Version 2.1*. Accessed: Dec. 9, 2018. [Online]. Available: <http://cvxr.com/cvx>.